CrossMark

Investigations on the structural, electrical and optical properties of thin films of CdO$_{(111)}$

M. Anitha[1] · V. Tamilnayagam[1,2] · N. Anitha[1] · L. Amalraj[1] · S. Gokul Raj[3]

Abstract Thin films of cadmium oxide (CdO) were prepared by simple nebulized pyrolysis technique by spraying on the amorphous glass substrates at five different volumes (5, 10, 15, 20 and 25 ml) of precursor cadmium acetate dihydrate solution. X-ray diffraction analysis reveals that the prepared films were oriented along with prominent (111) plane having cubic structure in CdO matrix. The surface morphology of these thin films showed sphere like structure was observed from scanning electron microscopic study. Transparency of these samples had decreased from 95 to 80% at longer wavelengths (900–1100 nm) with an increase in precursor solution volume. The energy band gap increases from 2.30 to 2.49 eV belonging to direct transition as the precursor solution volume had increased up to 20 ml and decreased for 25 ml. The presence of the absorption peak around 650 cm^{-1} corresponding to CdO bond was confirmed by FTIR spectrum. The emission spectrum of CdO thin films were investigated by fluorescence spectrum recorded at room temperature. Hall Effect measurement was carried out to investigate the electrical properties of the as deposited CdO thin films. The resistivity decreased from 36×10^{-2} to 7.54×10^{-3} Ω-cm and the activation energy (Ea) had decreased from 0.20 to 0.096 eV. The hot probe characterization proved, all these thin films were n-type semiconductor.

✉ L. Amalraj
amalraj57@yahoo.co.in

1 Department of Physics, V.H.N.S.N College (Autonomous), Virudhunagar, Tamilnadu 626001, India

2 Department of Physics, Arulmugu Palaniandavar College of Arts and Culture, Palani, Tamilnadu 624601, India

3 Department of Physics, C. Kandaswami Naidu College for Men, Chennai 600 102, India

1 Introduction

Thin films of zinc oxide (ZnO), tin oxide (SnO$_2$), indium oxide (In$_2$O$_3$) and cadmium oxide (CdO) were widely used as transparent conducting oxide (TCOs) thin films which finds applications in transparent electrodes, solar cells, phototransistors, optical heaters, opto-electronic deices and gas sensor applications [1–6]. Due to their high optical transmittance and electrical conductivity, it finds applications in flat display devices, aircraft windows and in optical communications [7–9]. CdO semiconductors belongs to II–VI group of n-type material with energy band gap of 2.5 eV [10, 11]. When compared with other semiconducting CdO possess low optical band gap; however CdO is a semiconductor oxide with high electrical conductivity and carrier mobility. There was several report on the CdO thin films which were prepared by various techniques out of which notably spray pyrolysis, sputtering, sol–gel were widely reported for their best prepared thin films. [12–20] Now-a-days thin film science has become a full fledged discipline because of the widespread applications of thin film devices in various fields which include optics, micro electronics, optoelectronic space science, defence, medical science, automobile industry and ornaments.

Nebulized spray pyrolysis method (NSP) is a simple and inexpensive method. Nebulizer is an instrument used by asthma patients. Nebulizer converts liquid into an aerosol. An aerosol is a suspension of small particles of liquid in a gas, where the sizes of the particle fall within the range of 1–5 micrometer in diameter. Similar kind of spray pyrolysis for TiO$_2$ compounds was also reported recently [21]. Advantage of NSP over conventional spray pyrolysis method is minimizing the wastage of precursor solution, less time consuming and enhanced quality thin films. These NSP technique were widely used for MgO [22], SnO$_2$ [23],

Cd doped SnO_2 [24], Nd doped ZnO [25], Sn doped ZnO [26] etc., of which most of them are either binary or ternary. The amount of deposition of layers can be varied when compared to the conventional pneumatic spraying system and it was reported by Mariappan et al. [26]. They found that the NSP possess many advantages of which low material consumption was biggest advantage and also they reported on the uniform layered thin films. The cost of the production was much cheaper and it was reported by Fu et al. [22]. To achieve more uniform thickness, other parameters such as solution concentration, substrate temperature, spray nozzle distance, pressure of carrier gas and volume of the solution can be easily adjusted to achieve enhanced film properties. Previous study has shown that the crystallinity of CdO films were strongly dependent on the growth conditions and thus its electrical properties can be modified [27]. Makori et al. [28] reported on the spray pyrolysis of 50 ml solution volume of the un-doped CdO thin films possess a resistivity of 42 Ω cm. There were also reports on the electrical and optical properties of un-doped CdO thin film (50 ml solution volume) which were deposited by spray pyrolysis method using perfume atomizer in which Usharani et al. [29] reported that the resistivity of 20 Ω cm with an optical band gap of 2.38 eV can be achieved.

In the present study, we report on the preparation of CdO thin films by nebulized spray pyrolysis and the enhancement of conductivity on the prepared CdO thin films with lesser volume of precursor solution were reported.
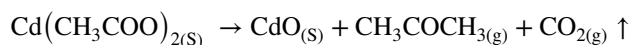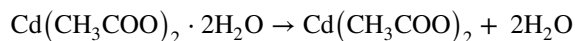
2 Experimental details

2.1 Materials and methods

In the present investigation spray pyrolysis technique was used to prepare the thin films of the CdO by the use of 0.2 M cadmium acetate dihydrate aqueous solutions [Cd(CH$_3$COO)$_2$]·2H$_2$O (99% Sigma-Aldrich) on the amorphous glass substrates with different precursor solution volume varying from 5 to 25 ml, in steps of 5 ml. The solution was sprayed manually using a nebulizer on preheated glass substrates. Cleaning of the glass substrates were done with chromic acid, double distilled water and acetone so that the CdO material adheres on the surface. The substrate temperature is controlled by using a chromel–alumel thermocouple. The solution volume is thus varied and simultaneously other deposition parameters such as substrate temperature, carrier gas, pressure and distance between glass tube & substrate were kept constant as 200 °C, 1.5 kg/cm^2 and 1 cm respectively. All the samples were kept safe in a desiccator to keep away from the moisture after removing them from the hot plate,

which was then cooled down so that it is maintained at room temperature.

The possible chemical reaction that takes place during deposition may be expressed as

$$Cd(CH_3COO)_2 \cdot 2H_2O \rightarrow Cd(CH_3COO)_2 + 2H_2O$$

$$Cd(CH_3COO)_{2(S)} \rightarrow CdO_{(S)} + CH_3COCH_{3(g)} + CO_{2(g)} \uparrow$$

The cadmium acetate in the aqueous solution transforms in to cadmium oxide and thereby the evolution of carbon-dioxide evolves as vapours.

2.2 Characterization technique

X-ray diffraction was carried out using XPERT PRO diffractometer to determine the crystal structure of the CdO thin films by using Cu Kα radiation (k = 1.5406 Å) with the range of angle between 20 and 70 degree in the scanning angle 2θ. Stylus profilometer was used to measure the thickness of the CdO thin films. The surface morphological studies were recorded with TESCAN VEGA-III scanning electron microscope (SEM) with a magnification of 25,000 which is fitted with the EDAX spectrum was recorded in the binding energy region 0–5 keV. Shimadzu-UV 1800 model was used to measure the transmittance spectra of these thin films was recorded in the wavelength range of 300–1100 nm using double beam spectrophotometer. The absorption spectral data was used to determine the type of optical transition and the band gap present in the sample. The reflectance spectrum of CdO thin films was recorded 200–900 nm in the wavelength region using UV-2400 PC Series. The IRAFFINITY-1 FTIR spectrometer was used to measure the Fourier transform infrared spectra (FTIR) in the wave number ranging from 600 to 1600 cm^{-1} for the experimental samples. The fluorescence spectra of CdO thin films were recorded using spectro fluorophotometer SHIMADZU RF-6000 in the wavelength ranging from 500 to 540 nm with an excitation at the wavelength of 325 nm. The resistivity of the samples was measured in the range 313–373 K in steps of 10 K by using four-point probe method. The semiconductor nature of this CdO thin film was verified by drawing Arrhenius plot with these data and the activation energy was calculated. HOT probe method was used to measure the conductivity of CdO semiconductor. Vander pauw method (Ecopia-HMS 3000) was used to measure the resistivity, mobility and carrier concentration of the experimental samples at room temperature.

3 Results and discussion

3.1 Film formation process

Amorphous glass substrates (of Borosil make) were used to deposit uniform, well-adherent with yellow colored CdO thin films. As the thickness is increased, the color of the film changed to dark brown from yellow which was also reported earlier by Salunkhe [30]. The thickness of the CdO thin films had increased from 420 to 530 nm due to the increase in
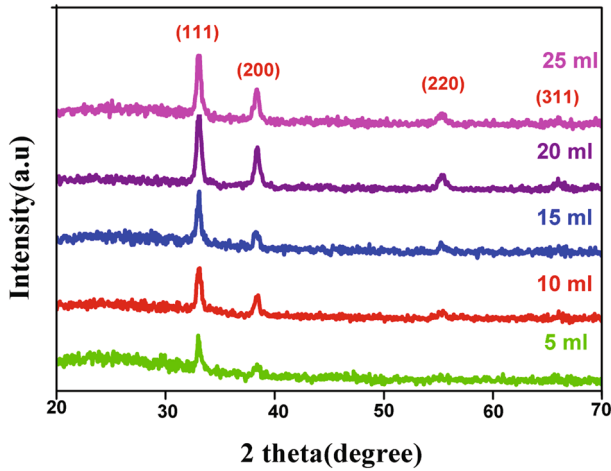
precursor solution volume of 5–20 ml and then decreases to 518 nm when solution volume is at 25 ml. Incomplete thermal decomposition causes a decrease in thickness while the powdery film formation due to homogeneous reaction also occurs. Spray pyrolysis techniques for the preparation of CdO thin films were also reported by Lokhande et al. [19].

3.2 X-ray diffraction pattern of CdO thin film

The XRD pattern of the prepared CdO thin films for different precursor solution volume is shown in Fig. 1. A strong peak at 33.03° corresponding to the miller planes (111) cubic structure, with other peaks at 38.5, 55.3, 65.8 and 69.3 due to (200), (220), (311) and (222) miller planes respectively were observed as shown in Table 1. The obtained diffraction peaks for all thin films were compared with the JCPDS value (File No. 05-0640). Pure CdO and In doped CdO thin films by spray pyrolysis method was reported by R. Kumaravel et al. which crystallized in similar cubic structure [20]. The Intensity of the peaks increases considerably as the precursor solution volume had increased up to 20 ml and then decreased as the precursor solution volume had further increased to 25 ml. These preliminary results indicate that the crystallinity of the CdO thin films had increased as the precursor volume had increased from 5 to 20 ml. This may be due to increase the film thickness. Then the crystallinity had decreased for 25 ml solution volume may be due to incomplete thermal decomposition reported in earlier.

Fig. 1 XRD patterns of CdO thin films coated at different precursor solution volume

Table 1 Structural parameters of CdO thin film at different precursor solution volume

Precursor solution volume (ml)	Thickness t (nm)	d-Spacing value (Å)		FWHM value (2θ)°	Orientation plane (hkl)
		Observed value (Å)	JCPDS value (Å)		
5	420	2.7156	2.7120	0.3936	(111)
		2.3337	2.3490	0.5904	(200)
10	487	2.7101	2.7120	0.3444	(111)
		2.3339	2.3490	0.3936	(200)
		1.6592	1.6610	0.5904	(220)
15	510	2.7106	2.7120	0.3444	(111)
		2.3553	2.3490	0.5904	(200)
		1.6636	1.6610	0.2952	(220)
20	532	2.7114	2.7120	0.2952	(111)
		2.3468	2.3490	0.1968	(200)
		1.6602	1.6610	0.2952	(220)
		1.4169	1.4160	0.4920	(311)
		1.3563	1.3555	0.5904	(222)
25	518	2.7120	2.7120	0.3444	(111)
		2.3490	2.3490	0.3444	(200)
		1.6610	1.6610	0.7872	(220)
		1.4169	1.4160	1.1808	(311)
		1.3563	1.3555	1.1808	(222)

Better crystallinity was observed for 20 ml precursor solution volume.

The size of the crystallite corresponding to prominent plane (111) was considered and was estimated using Debye Scherrer's formula [31]

$$D = \frac{0.9\lambda}{\beta \cos \theta} \qquad (1)$$

where 'β' corresponds to the full-width half maximum (FWHM) and 'λ' is the wavelength of X-ray used which is 1.5406 Å. As the precursor volume is increased to 20 ml, the size of the crystallites varies from 21.98 nm to 29.33 nm and then decreased for a solution volume of 25 ml [32]. The crystallite size calculated for the obtained CdO thin films for different solution volume shown in the Table 2. The decrement in the calculated D value is evident for the above mentioned degradation in the crystallinity.

The micro strain 'ε', dislocation density 'δ' lattice constant 'a', volume 'v' and number of crystallites (n) of the (111) peak was calculated from XRD data, using the relation [31] and tabulated in Table 2.

$$\varepsilon = \frac{\beta \cos \theta}{4} \qquad (2)$$

$$\delta = \frac{1}{D^2} \qquad (3)$$

$$\frac{1}{d^2} = \frac{h^2 + k^2 + l^2}{a^2} \qquad (4)$$

$$v = a^3 \qquad (5)$$

$$n = \frac{t}{D^3} \qquad (6)$$

Table 2 shows that the strain and dislocation density values initially decrease upto 20 ml and then increase with increasing precursor solution volume. For pure CdO

thin films prepared by spray pyrolysis by Velusamy et al. [31], it was found that the dislocation density (2.331×10^{15} lines/m^2) and strain value (1.68×10^{-3} lines^{-2} m^4). The higher values of crystallite size and lower value of strain and dislocation density indicate the higher crystalline properties and lower structural defects. The small value of 'δ' and 'ε' calculated for 20 ml of the precursor solution volume 1.162×10^{15} lines m^{-2} and 1.23×10^{-3} lines^{-2} m^4 in our present work through nebulized spray pyrolysis yields good quality polycrystalline CdO thin films. The calculated 'a' and 'v' value is in good agreement with the earlier reported values [32].

The fraction of layers undergoing sequence faults may be given as stacking faults probability (α*) in a given crystal and therefore, one fault is expected to be observed in (1/α*) layers. The stacking faults probability (α*) was calculated using the relation [33].

$$\alpha^* = \left(\frac{2\Pi^2}{45(3 \tan \theta)^{0.5}} \right) \beta \qquad (7)$$

The minimum stacking fault value is observed in 20 ml precursor solution volume shown in Table 2.

XRD patterns also revealed that change in precursor solution volume induces variation in CdO thin film texture. From the X-ray diffraction data, the texture coefficient Tc (h k l), of any particular plane can be calculated and may be given as below [31]

$$Tc(hkl) = \left[\frac{I(hkl)}{I_0(hkl)} \right] \Bigg/ \left\{ \frac{1}{N} \sum_i \left[\frac{I_i(hkl)}{I_0(hkl)} \right] \right\} \qquad (8)$$

where I_i (hkl) is the measured relative intensity, I_0 (hkl) is the standard intensity taken from the JCPDS data and N is the reflection number. The calculated Tc values are given in Table 2, which clearly indicates that the Tc value for (111) plane had increased from 1.633 to 1.98 with respect to the precursor solution volume had increased. Dakhel et al. also reported the texture coefficient value for (111) orientation of CdO thin film as 1.54 [34].

Table 2 Structural properties of prominent (111) plane of CdO thin film at different precursor solution volume

Precursor solution volume (ml)	Crystallite size (D) (nm)	Lattice Constant a=b=c (Å)	Unit cell volume v (Å)^3	Dislocation density δ × 10^{15} (lines/m^2)	Strain ε × 10^{-3} (lines^{-2} m^4)	Number of crystallites (n) × 10^{16} (m^{-2})	TC	Stacking fault (α*) × 10^{-3} (J/m^2)
5	22	4.694	103.42	2.070	1.646	3.944	1.633	3.19
10	25.13	4.704	104	1.583	1.440	3.21	1.65	2.79
15	25.14	4.686	103	1.582	1.440	3.07	1.77	2.79
20	29.33	4.694	103.42	1.162	1.234	2.11	1.98	2.39
25	25.13	4.700	103.42	1.583	1.440	3.26	1.73	2.79

3.3 Surface morphology and compositional analysis

The thin films of CdO were subjected to surface analysis to visualize its surface morphology with different precursor solution volume is shown in Fig. 2. The microstructure of all the thin films is homogeneous. The thin film deposited with 5 ml solution volume is seen to have sphere like structure with voids. The SEM image of the thin film coated
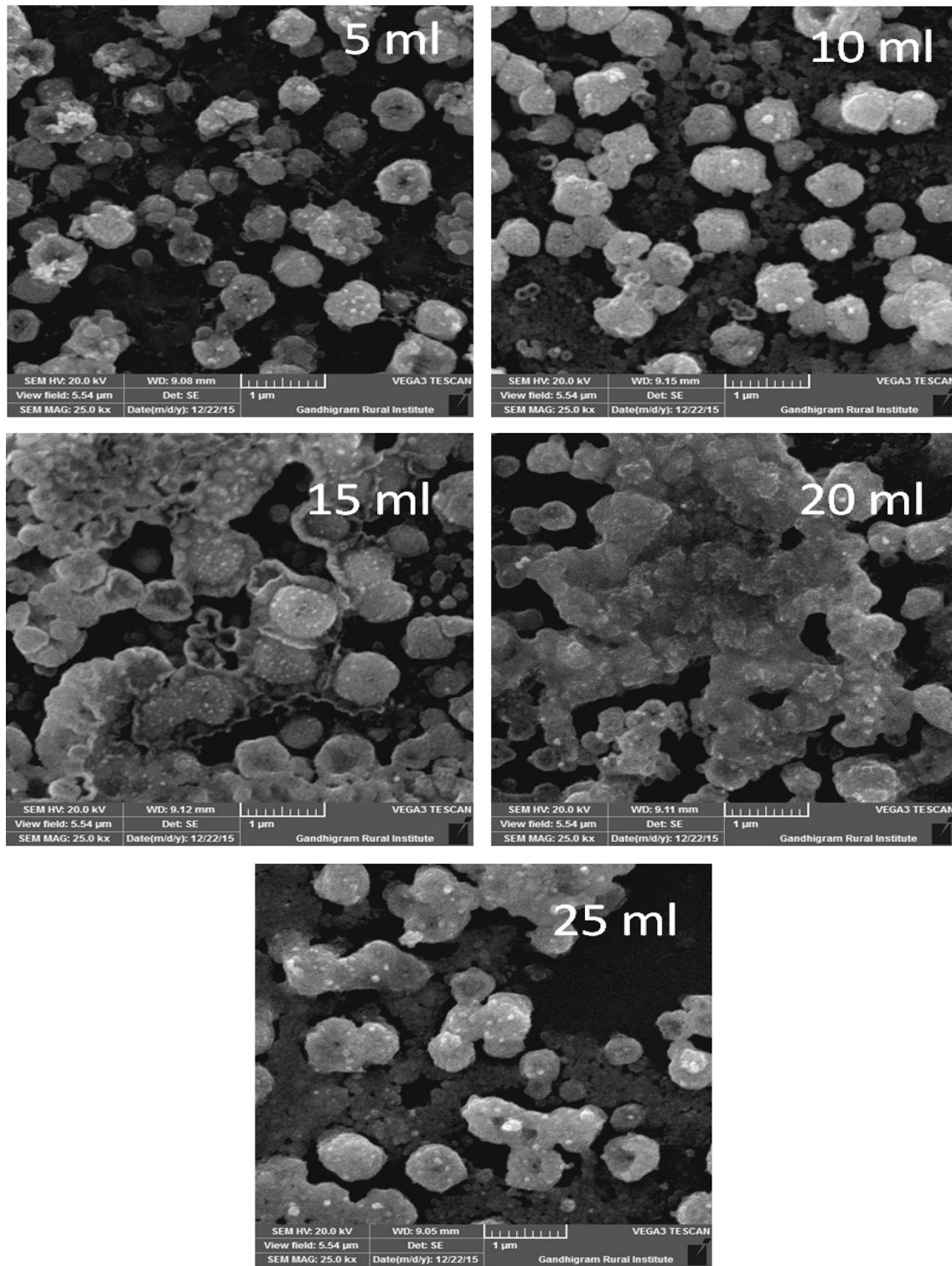

Fig. 2 SEM images of CdO thin films coated at different precursor solution volume

with 10 ml precursor solution volume looked similar but decreased voids and few grains are agglomerated. In the film coated with 15 ml precursor solution volume the surface appears to be densely packed with spherical shaped grains with most of grains are interconnected together. Agglomeration of grains for the thin film coated with 20 ml precursor solution volume seems to be complete and the surface appears to be tightly packed with spherical shaped grains for the CdO thin film. A similar result was observed by P.Velusamy et al. [31] for cerium doped CdO thin films which were formed by conventional by spray pyrolytic technique and Ravichandran et al. [35] for un-doped CdO nano particles synthesized by chemical precipitation method. As the precursor solution volume had increased to 25 ml the surface appears similar to the surface of the film deposited with 10 ml volume. This result may be attributed to the decrease in the thickness which resulted in reduced agglomeration. The average grain size had increased from 0.57 to 0.79 µm as the solution volume had increased from 5 to 20 ml. Then the grain size had decreased to 0.64 µm as the solution volume had increased to 25 ml. These variations of grain size correspond to the variation of thickness determined using styles profilometer and to the crystallite size determined using XRD analysis.

EDAX spectrum of CdO thin films deposited on the amorphous glass substrate at different solution volumes (not shown here as figure) confirms the presence of cadmium (Cd) and oxygen (O) elements without any other impurity [12]. For low precursor solution volume the atomic percentage of cadmium is low with the sheet resistance (R_{sh}) being maximum [36]. As the precursor solution volume increased, the atomic percentage of cadmium had increased; as a result, a decrease in sheet resistance (R_{sh}). For CdO thin film deposited with 25 ml precursor solution volume the cadmium percentage decreased, then the sheet resistance (R_{sh}) also increased. The silicon (Si) element appears to originate from the glass substrates [37].

3.4 Optical analysis

The transmittance spectrum of the prepared CdO thin films with different precursor solution volume is shown in Fig. 3a. The transmittance of all samples is minimum at a wavelength around 450 nm. They exhibited high transmittance (600–1100) in the visible as well as in IR region. The transmittance of CdO thin film had decreased from 93 to 84% in the visible region (900 nm) as the solution volume had increased from 5 to 20 ml. Then the transmittance had increased to 86% as the solution volume had increased to 25 ml. The transparency depends on the metal ions and also on the thickness of the formed thin films on the over the substrate. Generally metal rich thin films shows less transparency [38].
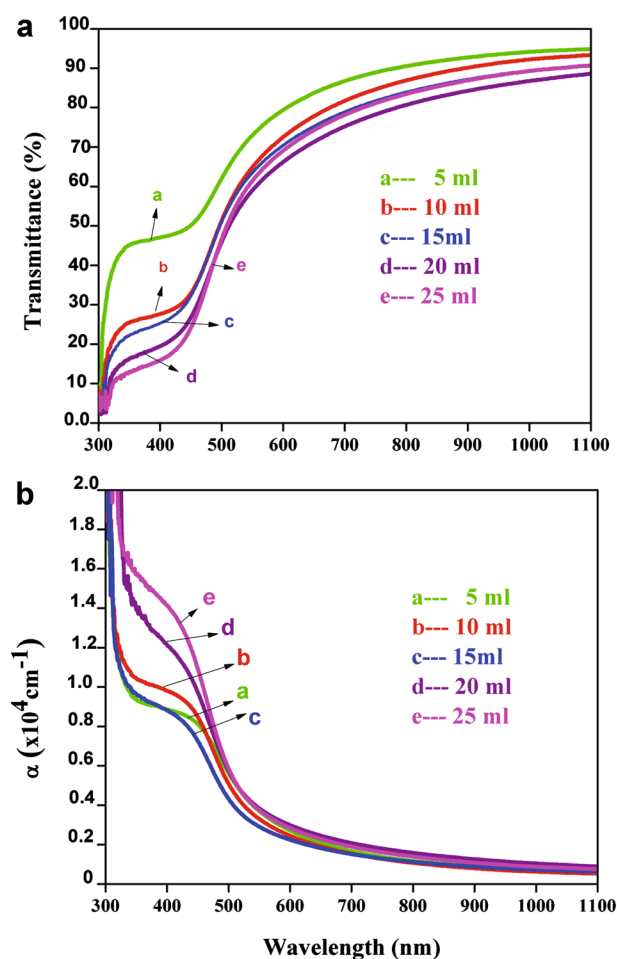

Fig. 3 a Transmittance spectrum and **b** absorption coefficient of CdO thin films coated at different precursor solution volume

Figure 3b shows the variation of wavelength with respect to the absorption coefficient (α) which is in the order of 10^5 cm^{-1} [16] and the calculation of absorption spectrum is plotted as shown in Fig. 3b. Maximum absorption coefficient of CdO thin films lies in the UV region around 350 nm wavelengths. There is an exponential decrease in the absorption as the wavelength increases from 600 to 1100 nm. The fundamental absorption edge was shifted towards the shorter wavelength as the precursor solution volume had increased, which may be correlated to the improvement of crystallinity, which is also revealed from XRD spectra.

Figure 4a shows the reflectance spectra of prepared CdO thin films. The reflectance of all samples minimum at a wavelength around 450 nm. They exhibited high reflectance (600–900) in the visible region. The reflectance of CdO thin film had increased from 9 to 10% in the visible region (900 nm) as the solution volume had increased from 5 to 20 ml. Then the reflectance had decreased to 9.5% as the solution volume had increased to 25 ml.
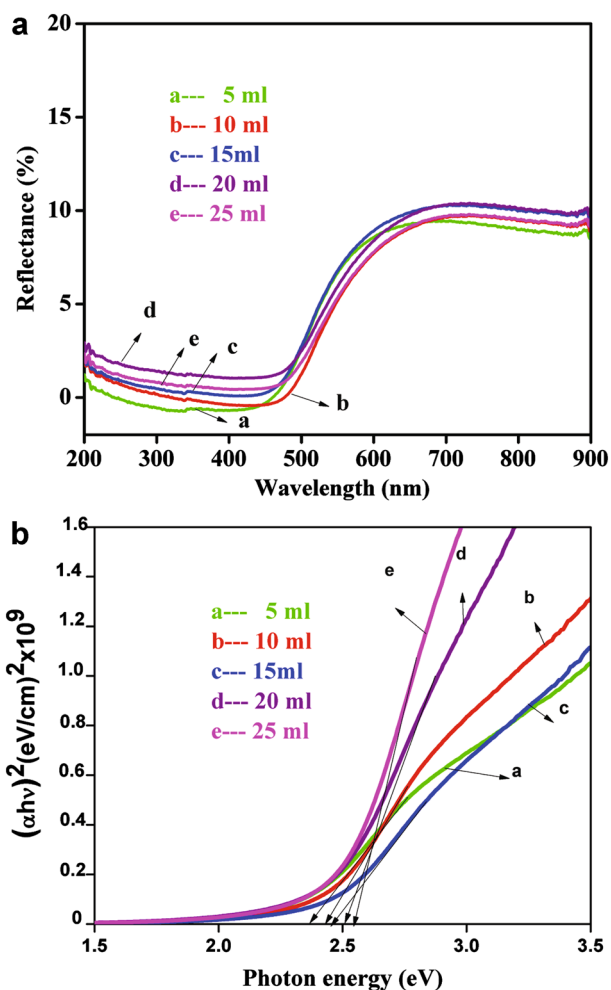
Fig. 4 a Reflectance spectrum and **b** plots of $(\alpha h\nu)^2$ vs. hν of CdO thin films coated at different precursor solution volume

Fig. 5 FTIR Spectrum of CdO thin films coated at different precursor solution volume

broadening is due to Moss–Burstein effect which is associated with the lifting of fermi level in which the conduction band of degenerate semiconductors leads to broadening of the energy band gap [41].

3.5 FTIR analysis

The FTIR spectrum of the prepared CdO thin films prepared for different precursor solution volume is shown in Fig. 5. The FTIR spectroscopy is the most common technique to study the chemical bond structure. The transmittance peak at 1450–1500 cm^{-1} may be assigned as the bending vibrations of CH$_2$. Kaviyarasu et al. [42] had reported the similar results. The peak at 1100 cm^{-1} is assigned to the C–O vibration band. The appearance of the weak absorption band at 680 cm^{-1} could be assigned to the Cd–O stretching (metal oxide) vibration. Thirumoorthi et al. also reported the peaks at 800–1400 cm^{-1} is assigned to CdO for Tin doping effect of CdO thin films prepared by spin coating method [43] and Trdjarodi et al. [44] had also reported 675 cm^{-1} indicates the formation of cadmium–oxygen phase for CdO spherical nano particles.

3.6 Fluorescence study

A fluorescence study of CdO thin films for different precursor solution volumes is shown in Fig. 6. The increase in the precursor solution volume increases the peak intensity of the CdO thin films (5–20 ml) and then it decreased to 25 ml solution volume. The emission spectra of all CdO thin films excited at 325 nm reveal one sharp band around 520 nm which is due to the oxygen deficiencies of CdO and also due to the recombination of a photo generated hole in

The energy band gap of all the thin films was determined using the Tacu's (arhenius) relation [39]

$$(\alpha h\nu) = A \left(h\nu - E_g \right)^p \tag{9}$$

where E_g is the band gap energy, A is a constant quantity, p has a discrete value like 1/2 or 2 depending on whether the transition is direct or indirect, α is the absorption coefficient, h is the Plank's constant and ν is the frequency of transmitted light. It can be clearly seen that the prepared CdO thin films are directly allowed semiconducting materials and thus confirms the experimental results and also from the theoretical calculations [40]. $(\alpha h\nu)^2$ versus hν values were plotted as shown in Fig. 4b in order to find out the direct band gaps respectively. The optical band gap values had increased from 2.30 to 2.49 eV as the precursor solution volumes had increased and then decreased 2.47 eV for higher precursor solution volume. Thus increased solution volume widens the optical energy band gap (Eg). This energy band gap (Eg)
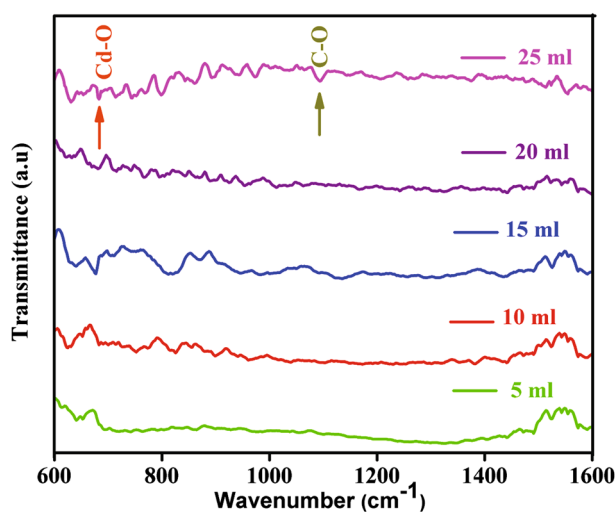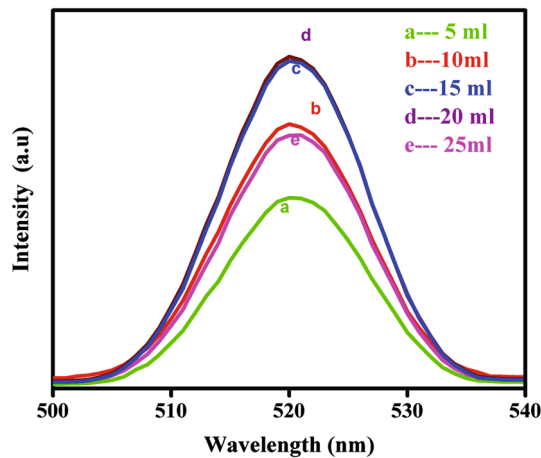
Fig. 6 Fluorescence spectrum of CdO thin films coated at different precursor solution volume

valence band with which it causes an electron in the conduction band [44, 45]. The linear increase in the intensity of the green emission (up to 5–20 ml) is due to the increase of the precursor solution volume and then decreased for 25 ml solution volume. These results are in consistent with the XRD result mentioned above. The energy band gap (Eg) can be calculated using the relation,

$$E_g = \frac{hc}{\lambda} \quad (J). \tag{12}$$

The energy band gap (Eg) of the prepared thin films of CdO are estimated from the fluorescence spectrum 2.38 eV (green emission) and found to be coinciding with the values observed from the optical study.

3.7 Electrical properties

The electrical measurements are determined by four probe measurement systems. The activation energy of the CdO thin films can be found by electrical resistivity plots shown in Fig. 7. The activation energy is an important tool for evaluating the position of Fermi levels in a pure semiconductor material. The activation energy is calculated from the slope of the line shown in Fig. 7, for the five samples and their values are given in Table 3. The activation energy values E_a are calculated using the relation [46].

$$\rho = \rho_0 \exp\left(\frac{E_a}{kT}\right) \tag{13}$$

where "k", be the Boltzmann constant, "ρ_0" is a parameter and "T" be the temperature in Kelvin. The activation energy of CdO thin film had decreased from 0.30 to 0.094 eV as the precursor solution volume had increased from 5 to 20 ml and then increased for 25 ml. Bhosale et al. also reported the

activation energy 0.077 eV for prepared CdO thin films by spray pyrolysis technique [47]. The hot-probe technique is a very simple technique to find the difference between n-type and p-type semiconductors. The prepared CdO thin films were found to have n-type semiconducting nature.

The variation in carrier concentration, electrical resistivity and mobility of CdO thin films prepared at different precursor solution volume is shown in Fig. 8. The resistivity had decreased from 70.1×10^{-3} Ω cm to 7.54×10^{-3} Ω cm as the solution volume had increased from 5 to 20 ml. This result may be attributed to the percentage of cadmium present in the samples, which is also in good agreement with that of the EDAX results of the CdO thin film prepared with 5 to 20 ml solution volume. Then the resistivity had increased to 12.6×10^{-3} Ω cm as the solution volume had increased to 25 ml which is due to the cadmium percentage being decreased. The low resistivity value 7.54×10^{-3} Ω-cm obtained from 20 ml solution volume for the CdO thin film, matches with the value obtained by Dakhel et al. [48] for the un-doped CdO thin film prepared by perfume atomizer using spray pyrolysis technique.

3.8 Opto-electronic properties

3.8.1 Figure or merit (FOM)

The figure of merit is an important parameter in optoelectronic application. In this work, to analyze the optoelectronic performance of different volume precursor solution of CdO thin films, the FOM values were calculated using the formula [49].

$$FOM(\Phi_{TC}) = \frac{T^{10}}{R_{sh}} \tag{14}$$

Where T^{10} is the optical transmittance and R_{sh} is the sheet resistance of CdO thin films. Figure of merit (FOM) values for the as prepared CdO thin films at different precursor solution volumes are listed in Table 3. It can be seen that the prepared thin films of CdO with 20 ml volume has a high figure of merit (6×10^{-3} Ω^{-1}). Velusamy et al. [31] had reported the similar FOM value of 1.0×10^{-3} Ω^{-1} for un-doped CdO thin film. Thus the result show that the thin film prepared with 20 ml precursor solution volume has high figure of merit and high electrical conductivity.

4 Conclusion

Thin films of cadmium oxide (CdO) on amorphous glass substrate with yellow color were prepared by nebulized spray pyrolysis technique with different precursor solution volume. The effect of thickness on morphology,
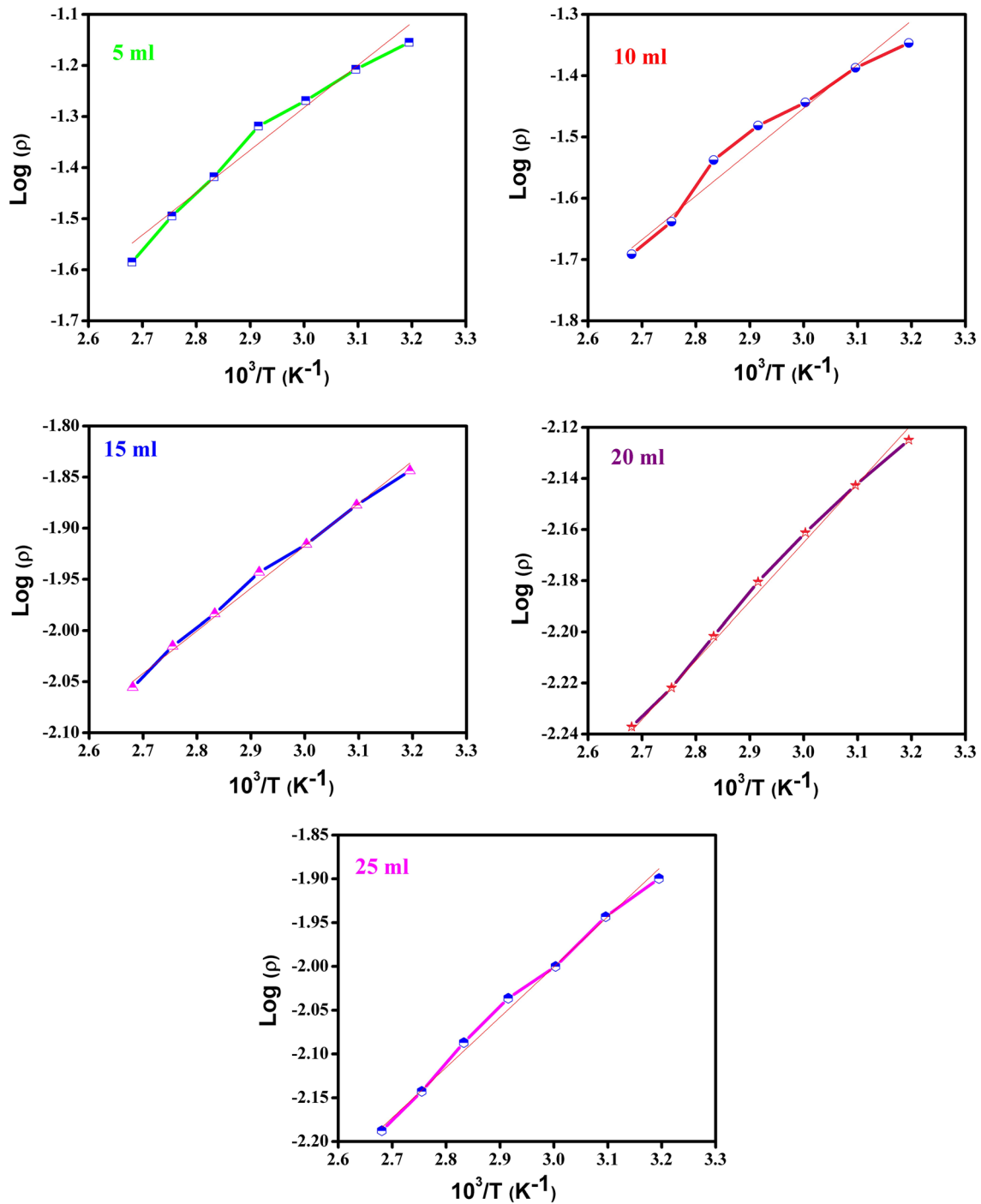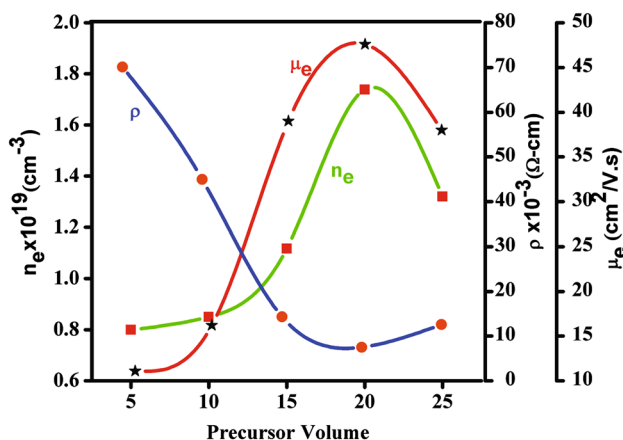
Fig. 7 Electrical resistivity plots of CdO thin films coated at different precursor solution volume

crystal structure, bonding confirmation, optical band gap and electrical resistivity of the prepared thin films were investigated in detail. Thin film XRD diffraction patterns confirms the formation of polycrystalline films in the cubic crystal structure with a preferential orientation along the (111) plane. Transmittance spectrum reveals the optical transparency in the formed thin films and that the energy band gap (E_g) increases from 2.3 to 2.5 eV with increase in precursor solution volume. The FTIR spectrum identified the presence of cadmium and oxygen very strongly bonded. The CdO thin film has good optical properties and hence it is a promising candidate for the optoelectronic devices. A minimum electrical resistivity of $7.54 \times 10^{-3} \, \Omega \, cm$ with activation energy of 0.09 eV was

Table 3 Electrical properties of CdO thin films at different precursor solution volume

Precursor solution volume (ml)	Sheet resistance $(R_{sh}) \times 10^3$ (Ω/sq)	Activation energy (E_a) (eV)	Conductivity (σ) (Ω-cm)$^{-1}$	Figure of merit $(\Phi_{TC}) \times 10^{-3}$ (Ω^{-1})	Reference work
5	1.6	0.20	14.29	0.5	Present work
10	0.92	0.15	22.22	0.98	Present work
15	0.28	0.13	69.78	3.11	Present work
20	0.14	0.09	132.63	6.0	Present work
25	0.24	0.18	79.37	3.58	Present work
60	234.24	–	–	–	SP [42]

Fig. 8 The variation of carrier concentration, electrical resistivity and mobility of CdO thin films at different precursor solution volume

determined for the film prepared with a solution volume of 20 ml.

References

1. M. Ito, Y. Sato, P.K. Song, A. Kaijio, K. Inoue, Y. Shigesato, Thin Solid Films **496**, 99–103 (2006)
2. J.T. Lim, C.H. Jeong, A. Vozny, J.H. Lee, M.S. Kim, G.Y. Yeom, Surf. Coat. Tech. **201**, 5358–5362 (2007)
3. A.K. Kulkarnia, C.H. Kirk, T.S. Lima, M. Khanb, Thin Solid Films **345**, 273–277 (1999)
4. J.I. J.Tores, G.G. Cisseneros, F. Alvarez, Thin Solid Films **289**, 238–241 (1996)
5. V.M. Nikale, C.H. Bhosale, Solar Energy Matter. **82**, 3 (2004)
6. D.V. Morgan, Y.H. Aliya, R.W. Bunce, A. Salehi, Thin Solid Films **321**, 268–272 (1998)
7. Y. Zhu, R.J. Mendelsberg, J. Zhu, J. Han, A. Anders, Appl. Surf. Sci. **265**, 738 (2013)
8. N. Rajesh, J.C. Kannan, S.G. Leonardi, G. Neri, T. Krishnakumar, J. Alloys Compd. **607**, 54–60 (2014)
9. Z. Zhao, D.L. Morel, C.S. Ferekides, Thin Solid Films **413**, 203–211 (2002)
10. N. Manjula, K. Usharani, A.R. Balu, V.S. Nagarethinam, Int. J. Chem. Tech. Res. **6**, 705–718 (2014)
11. A.A. Ziabari, F.E. Ghodsi, G. Kiriakidis Surf. Coat. Technol. **213**, 15–20 (2012)
12. L. Balakrishnan, S. Gokul Raj, S.R. Meher, K. Asokan, Z.C. Alex, Appl. Phys. A **119**, 1541–1553 (2015)
13. B. Sahin, T. Taskopru, F. Bayansal, Ceram. Int. **40**, 8709–8714 (2014)
14. R.J. Y.Zhu, J. Mendelsberg, J. Zhu, A. Han, Anders, J. Mater. Sci. **48**, 3789–3797 (2013)
15. D.S. Dhawale, A.M. More, S.S. Latthe, K.Y. Rajpure, C.D. Lokhande, Appl. Surf. Sci. **254**, 3269–3273 (2008)
16. A.J. Varkey, A.F. Fort, Thin Solid Films **239**, 211–213 (1994)
17. J.S. Cruz, G.T. Delgado, R.C. Perez, C.I.Z. Romero, O.Z. Angel, Thin Solid Films **515**, 5381–5385 (2007)
18. B. Saha, R. Thapa, K.K. Chattopadhyay, Solar Energy Mater. **92**, 1077–1080 (2008)
19. B.J. Lokhande, P.S. Patil, M.D. Uplane, Mater. Chem. Phys. **84**, 238–242 (2004)
20. R. Kumaravel, K. Ramamurthi, V. Krishnakumar, J. Phy. Chem. Sol. **71**, 1545–1549 (2010)
21. V. Tamilnayagam, P. Jegatheesan, K. Pakiyaraj, L. Amalraj, J. Mater. Sci. **27**, 11530–11535 (2016)
22. X. Fu, F. Wu, S. Song, X. Duo, C. Lin, Appl. Surf. Sci. **148**, 223–228 (1999)
23. P. Thiruramanathan, G.S. Hikku, T. Ramkumar, L. Amalraj, J. Adv. Phys. **5**, 1–3 (2016)
24. R. Mariappan, V. Ponnuswamy, P. Suresh, Mater. Sci. Semicond. Process **16**, 825–832 (2013)
25. T. Prasada Rao, S. Gokul Raj, M.C. Santhosh Kumar, Proce. Mater. Sci. **6**, 1631–1638 (2014)
26. R. Mariappan, V. Ponnuswamy, P. Suresh, Superlattices Microstruct. **52**, 500–513 (2012)
27. V. Gowthami, P. Perumal, R. Sivakumar, C. Sanjeeviraja, Phys. B Condens. Matter. Phys. **452**, 1–6 (2014)
28. N.E. Makori, I.A. Amatalo, P.M. Karimi, W.K. Njoroge, Int. J. Optoelectron. Eng. **4**, 11–15 (2014)
29. K. Usharani, A.R. Balu, V.S. Nagarethinam, M. Suganya, Prog. Nat. Sci. **25**, 251–257 (2015)
30. R.R. Salunkhe, D.S. Dhawale, D.P. Dubal, C.D. Lokhande, Sens. Act. B **140**, 86–91 (2009)
31. P. Velusamy, R. Ramesh Babu, K. Ramamoorthy, M.S. Dahlem, E. Elangovan, RSC Adv. **5**, 102741–102749 (2015)
32. A. Khorsand Zak. W.H.A. Majid, M.E. Abrishami, R. Yousefi, Solid State Sci. **13**, 251–256 (2011)
33. S.J. Helen, S. Devadason, T. Mahalingam, J. Mater. Sci. **27**, 4426–4432 (2016)
34. A.A. Dakhel, Thin Solid Films **518**, 1712–1715 (2010)
35. A.T. Ravichandran, A. Robert Xavier, K. Pushpanathan, B.M. Nagabhushana, R. Chandramohan, J. Mater. Sci. **21**, 2693–2700 (2015)
36. A. Bagheri Khatibani, S.M. Rozati, Z.A. Hallaj, Mater. Sci. Semicond. Process **16**, 980–986 (2013)
37. S. Kose, F. Atay, V. Bilgin, I. Akyuz, Int. J. Hydrog. Energy **34**, 5260–5266 (2009)

38. L.R. de Leon-Gutierrez, J.J. Cayente-Romero. J.M. Peza-Tapia, E. Barrera-Calva, J.C. Martinez-Flores, M. Ortega-Lopez, Matter. Lett. **60**, 3866–3870 (2006)

39. K. Usharani, N. Raja, N. Manjula, V.S. Nagarethinam, A.R. Balu, Int. J. Thin Films Sci. Tecnol. **2**(4), 89–96 (2015)

40. A.A. Dakhel, Mater. Chem. Phys. **130**, 398–402 (2011)

41. E. Burstein, Phys. Rev. B **93**, 632–633 (1954)

42. K. Kaviyarasu, E. Manikandan, P. Paulraj, S.B. Mohamed, J. Kennedy, J. Alloy Compd. **593**, 67–70 (2014)

43. M. Thirumoorthi, J.T.J. Prakash, J. Asian Ceram. Soc. **4**, 39–45 (2016)

44. A. Tadjarodi, M. Imani, H. Kerdad, Int. Nano Lett. **43**, (1–6) (2013)

45. T. Jun kuo, Z. Micheal, H. Huang, J. Phys. Chem. B **110**, 13717–13721 (2006)

46. L. Amalraj, M. Jayachandran, C. Sanjeeviraja, Mater. Res. Bull. **39**, 2193–2201 (2004)

47. C.H. Bhosale, A.V. Kambale, A.V. Kokate, K.Y. Rajpure, Mater. Sci. Eng. B **122**, 67–71 (2005)

48. A.A. Dakhel, Opt. Mater. **31**, 691–695 (2009)

49. N. Ravichandran, T. Dineshbabu, A. Arun. E. Manivasaham, E. Sindhuja, Appl. Surf. Sci. **392**, 624–633 (2017)